

# DYNAMIC PROPERTIES OF PRE-ALLOYED MO-STEEL POWDERS FOR HIGH-LOADED P/M APPLICATIONS

Guido Olschewski, QMP Metal Powders GmbH, Mönchengladbach/Germany  
Denis Barrow, QMP Metal Powders Ltd, Ipswich/England

## Abstract

*In order to maintain its competitive edge, the P/M industry needs high-strength materials and components that can be manufactured at low cost, for example, sintered steels for highly stressed safety components in the automobile. The employment of sintered steels is, however, frequently impaired by their production-specific residual porosity, which affects dynamic properties. The objective of a project by QMP Metal Powders GmbH was to develop and optimise new, pre-alloyed molybdenum steel powders that can be used to manufacture sintered components of high density P/M parts. The pre-alloyed molybdenum steel powder MSP 3.5 Mo was improved with regard to its strength and toughness properties. MSP 3.5 Mo is characterised by its very high density of 7,5 g/cm<sup>3</sup> as a result of sintering in the  $\alpha$ -phase. High elongation and notch impact energy values can be achieved.*

**Keywords:** *high density P/M parts,  $\alpha$ -phase sintering, pre-alloyed Mo-steel powders*

## 1. Introduction

The implementation of P/M components in automotive applications increases continuously. Especially applications in heavy-duty components like gears, pistons and connecting rods that are exposed high cycle dynamic loads can be realised with new developed materials [1]. It is known that the dynamic properties of P/M parts are a complex phenomena which are influenced by numerous factors like pores, microstructure, heat treatment, etc. [2]. In several studies it has been proved that the porosity of a P/M part has the greatest influence [3, 4]. It can generally be assumed that raising the density leads to a more or less linear increase of the static mechanical properties, while the fatigue and impact strength increase exponentially [5]. A conventional method of attaining high component density is shrinkage during sintering. The most effective way of increasing shrinkage with sintered steels is to execute sintering in the ferritic phase ( $\alpha$ -phase). In the ferritic phase, the diffusion coefficient of Fe is approximately 100 times higher than in the austenitic phase ( $\gamma$ -phase). The self-diffusion of iron in iron can be calculated as follows [6]:

$$D = D_0 \cdot \exp\left(\frac{-\Delta H_D}{kT}\right)$$

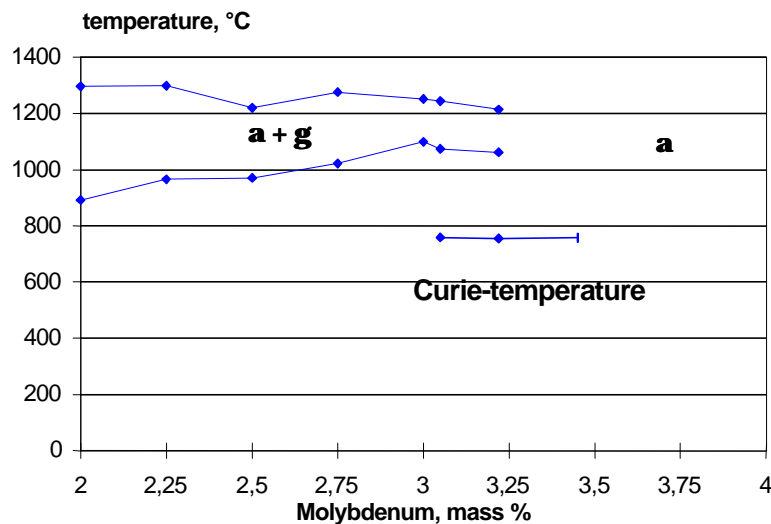
- $D$  = diffusion constant in cm<sup>2</sup>/s
- $D_0$  = material-dependent diffusion constant in cm<sup>2</sup>/s
- $\Delta H_D$  = activation energy in eV
- $k$  = Boltzmann constant =  $1.38062 \times 10^{-23}$  J/K
- $T$  = temperature in K

This finding inspired the development of the QMP MSP 3.5 Mo water atomised, pre-alloyed steel powder with a molybdenum content of 4.0 wt-%. Because of this molybdenum content the sintering behaviour of the material is constant during the high temperature sintering process. The outstanding property of this material is the component density of 7.5 to 7.6 g/cm<sup>3</sup> (approx. 95% of the theoretical density) that can be achieved by single sintering without a liquid phase.

## 2. Establishing suitable alloy systems

The fact that molybdenum extends the ferritic zone of iron is known in literature. Therefore the Fe-Mo system seems promising for P/M materials sintering exclusively in the  $\alpha$ -phase. The Fe-Mo phase diagram was established on the basis of dilatometric tests and thermodynamic calculations. As the material MSP 3.5 Mo is to sinter fully in the  $\alpha$ -phase, knowledge of the exact boundaries of the different phases is indispensable. A phase diagram can be designed by means of dilatometric curves, see figure 1.

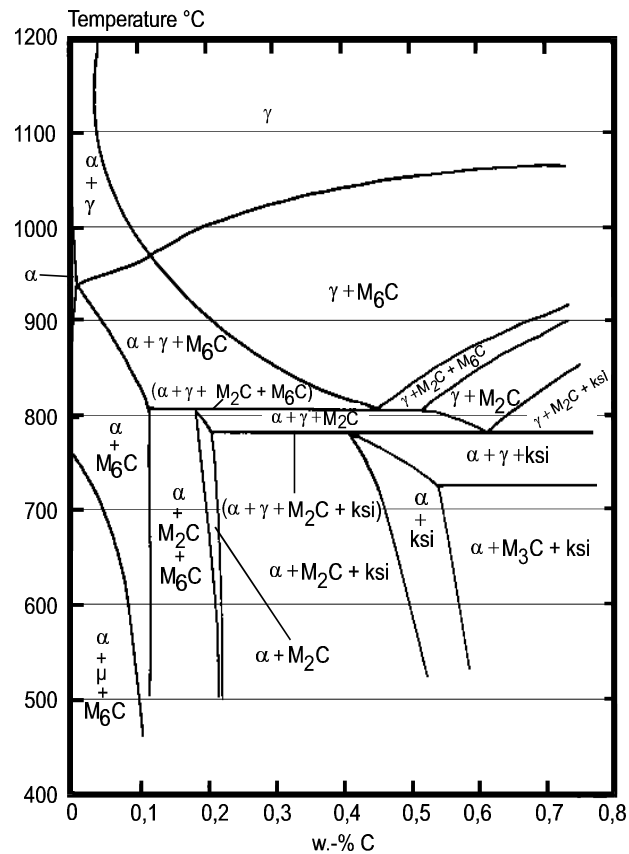
Fig. 1. Fe-Mo phase diagram established on the basis of dilatometric curves



With rising molybdenum content, the phase region  $\alpha + \gamma$  is increasingly restricted. Up to a molybdenum content of 3.5 mass-%, a phase transformation  $\alpha \rightarrow \alpha + \gamma \rightarrow \alpha$  takes place while the material is heating up. With a molybdenum content of 4.0%, the dilatometer printouts did not show any transformation. With this Mo-content, the material is purely ferritic over the entire temperature range. The programs Chemsage and Thermocalc of the Institute of Ferrous Metallurgy (RWTH Aachen/Germany) [7] were used to calculate the ternary phase diagram Fe-Mo-C. On the one hand, the diagram is intended to provide information on the stability of the  $\alpha$ -phase during carbon-free processing. On the other hand, the purpose of the calculation was to clarify how much of the alloying element carbon may be added at the very most to achieve nothing but the ferritic phase during the

sintering process. In addition, the various phases undergone by the material in the course of case hardening, as a function of the austenitising temperature, were to be demonstrated.

**Fig. 2.** Quasi-binary section through the Fe-Mo-C phase diagram at a molybdenum content of 3.5 mass-%



The effect of carbon on the Fe-Mo system is extremely complex. For the Fe-Mo-C phase diagram, quasi-binary sections at 3.5 mass-% were calculated (figure 2). The molybdenum content was kept constant in each case to avoid complicating the diagrams unnecessarily. On the one hand, the  $\alpha$ -zone is extremely restricted by carbon, with a maximum possible extension of the  $\alpha$ -phase up to around 940°C and approximately 0.01% carbon. Sintering must therefore be practically carbon-free in order to take advantage of effect of the high self-diffusion coefficient of iron in the  $\alpha$ -phase. Carbon should therefore be introduced into the material after sintering, for example by case hardening. On the other hand, the phase diagram shows that the usual austenitising temperatures of 850 – 950°C are not sufficient to decompose the  $M_6C$  carbides and to austenitise the material completely. Case hardening must be done at temperatures above 1050°C in order to avoid carbide precipitation.

The strength of MSP 3.5 Mo at about 350 MPa is still low. Therefore niobium and phosphorus were added to the basic powder to increase its strength. These elements do not constrict the ferritic phase. It was found out that merely partial alloying with phosphorus improves strength with elongation after fracture it's remaining the same. Niobium also seems promising although its strength-increasing effect only shows after carbon is added by a thermochemical treatment (case hardening), but not in the as-sintered condition.

### 3. Optimisation of case hardening

The solution temperature of the carbides is essential for case hardening since carbides at the grain boundaries substantially reduce strength and toughness properties. If low austenitising temperatures are selected for case hardening, figure 2 shows that special carbides of the  $M_6C$  type appear at the grain boundaries. The decomposition of the carbides can be subdivided into different stages. At an annealing temperature of 900°C (figure 3), the carbide network still exists, but the carbides already start to coalesce as round structures (1<sup>st</sup> stage). The 2<sup>nd</sup> stage emerges after an annealing treatment at 1000°C. Now nothing but round, coalesced and coagulated carbides are visible. In the 3<sup>rd</sup> stage, individual carbides start to disintegrate, and from a temperature of 1050°C the percentage of carbides decreases noticeably. If an annealing temperature above 1100°C is selected, all carbides will disintegrate, see figure 4.

Fig. 3. Annealing temperature of 900°C:  
carbide network at the grain boundaries  
X = 1000

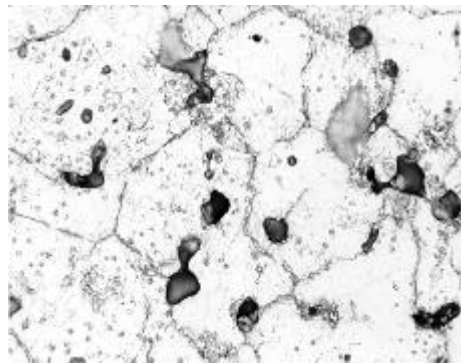
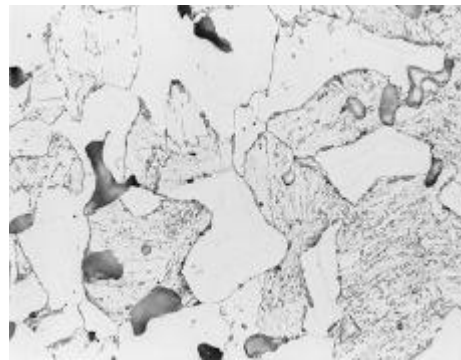


Fig. 4. Annealing temperature of 1100°C:  
carbides have disintegrated  
X = 1000



Therefore an austenitising temperature of more than 1050°C must be chosen for case hardening to prevent the formation of special carbides at the grain boundaries. Subsequently, case hardening treatments including plasma carburising were carried out. The microstructure was examined by light-optical and scanning electron microscope, and the effective case depth over the sample width measured to DIN 30 911. By case hardening, the hardness of the case can be increased significantly, since as a result of the introduction of carbon and the subsequent quenching the microstructure is transformed from ferrite into martensite.

Fig. 5. Ferritic microstructure free from carbides

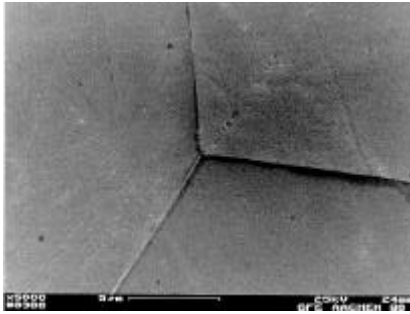
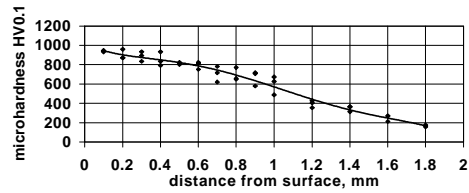


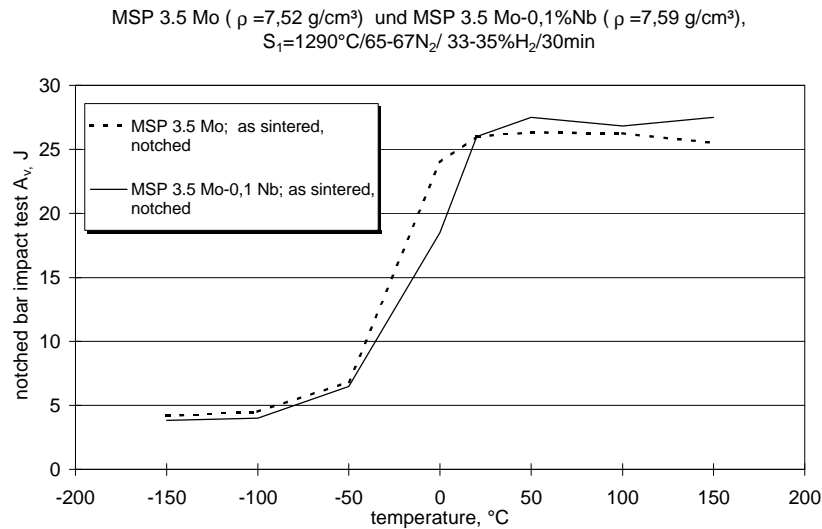
Fig. 6. Variation in hardness through the case hardened layer, MSP 3.5 Mo ( $T_{\text{aust}} = 1080^{\circ}\text{C}$ , direct hardening treatment:  $900^{\circ}\text{C}$ )



With the samples that were directly hardened at an austenitising temperature of  $1080^{\circ}\text{C}$  or above, hardly any carbides were formed at the grain boundaries, as shown in figure 5. Even in 5000-fold magnification by the SEM, no carbides are visible at the grain boundaries. Then the influence of the temperatures of the direct hardening treatments on carbide formation and variations in hardness was compared.

A high case hardness of more than 900 HV 0.1 was determined, with even variations in hardness, as represented in figure 6. Therefore samples were case hardened at an austenitising temperature of  $1080^{\circ}\text{C}$ , followed by direct hardening at  $900^{\circ}\text{C}$ .

Fig. 7.  $A_v$ -T graphs, sintering condition



#### 4. Results of notched bar impact bending tests and impact bending tests

The impact bending tests and notched bar impact bending tests were run to DIN EN 10 045, at test temperatures ranging from +150°C to -150°C. The unnotched samples were produced to DIN ISO 5754, and the notched ones provided with a V-notch to DIN EN 10 045. The direction of the impact was to be perpendicular to the compacting direction. At first, samples of the materials MSP 3.5 Mo and MSP 3.5 Mo-0.1Nb were tested in as-sintered condition, see figure 7.

The graphs clearly show the transition from lower shelf energy to upper shelf energy. The  $A_v$ -T graphs of the both variants almost coincide; the impact transition temperature  $T_{Avmax/2}$  is reached at approximately 0°C. In the as-sintered condition, the microalloying element niobium does not have any measurable effect on toughness. At low temperatures transcrystalline cleavage fracture occurs, see figure 8.

In the upper shelf, the fracture occurs as shear fracture after plastic deformation as a result of the formation of cavities around impurities or inclusions. Additional deformation causes those cavities to grow, and the ligaments between the cavities to be cut off. The resultant fracture surface is of an alveolate appearance, see figure 9.

Fig. 8. Transcrystalline cleavage fracture of MSP 3.5 Mo at -150°C

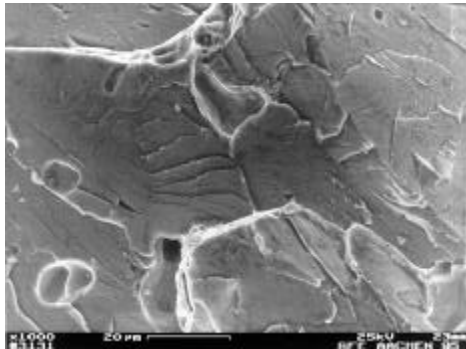
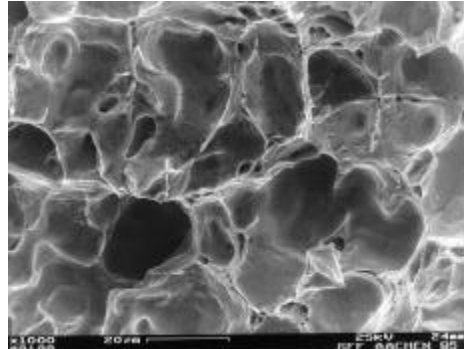


Fig. 9. Shear fracture surface of surface of MSP 3.5 Mo at +150°C



The next step consisted of austenitising the MSP 3.5 Mo at 1080°C and hardening the material directly at 900°C. Figure 10 shows load-deflection curves of the material MSP3.5Mo in the as-sintered condition and in case hardened condition. They were established on unnotched samples at room temperature (MSP 3.5Mo, case hardened) and at 0°C (the as-sintered condition). For the material MSP 3.5Mo in the as-sintered condition, crack initiation, stable crack propagation with plastic deformation and eventually the fracture can be clearly distinguished by the curve shape. High deflections are attained before the fracture occurs; the material is of ductile behaviour. As a result of case hardening, the deflection before fracture decreases sharply, while the maximum force increases. Only unstable crack extension occurs.

Case hardening greatly decreases impact energy values, which are essentially determined by the deflection occurring before unstable crack extension begins, over the entire temperature range. Toughness is significantly influenced by the microstructure, as the porosity of the material MSP 3.5Mo is the same in as-sintered and case hardened condition,

and no grain boundary carbides are present. During examinations of fractures by means of SEM, different fracture mechanisms were detected in the case hardened case area and the sample centres.

Fig. 10. Load-deflection curves of the material MSP 3.5 Mo in as-sintered and in case hardened condition

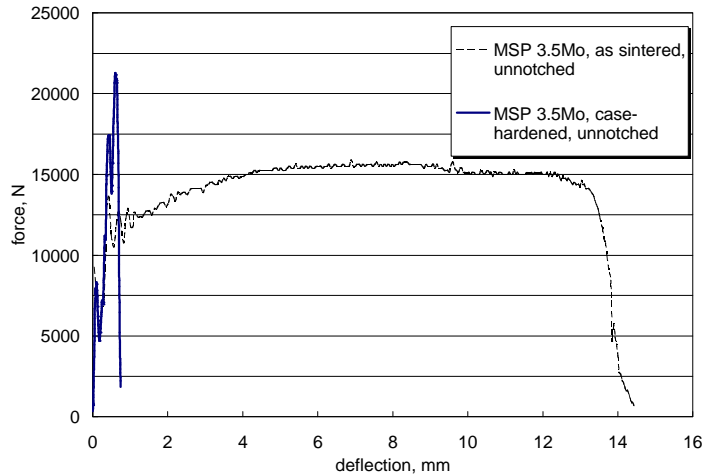


Figure 11 shows the fracture surface in the case area of a sample broken at room temperature: It is of a deeply fissured appearance, with irregular plateaux. This is a quasi-cleavage fracture frequently found in tempered martensite. In materials with intergrown mixed microstructures or of flaky and acicular microstructural composition, e.g. bainite or martensite, the individual cleavage planes are formed differently, depending on their type and the degree of bonding. Here, separation no longer occurs exclusively on the low-indexed cleavage planes but also along the higher-indexed crystal lattice planes. In addition, separations can take place along the boundary surfaces of intergrown flakes and aciculae. In the middle of the sample, cleavage fracture and shear fracture occur side by side, see Figure 12. In this area, the microstructure is purely ferritic. There are no carbide precipitations at the grain boundaries.

## 5. Results of the fatigue strength test

The  $P_s$  50% probabilities of survival of the materials tested under axial load and deflection ( $R = 0$  and  $R = -1$ ) are represented in Figure 11 and Figure 12. Independently of alloy composition, sintering and heat treatment parameters, higher fatigue strengths are achieved under bending load than under axial load. Under a bending load, a stress gradient exists in the material. Only the sample case has to bear the maximum stress, whereas with an axial load the entire sample cross-section is subjected to the maximum load. Also, higher fatigue resistance values are attained under alternating load ( $R = -1$ ) than under pulsating load ( $R = 0$ ), since there is no mean load in this case, i.e. the absolute stress is lower.

Fig. 11. Reproduction of a fracture in the case area of a case hardened sample (T = RT)

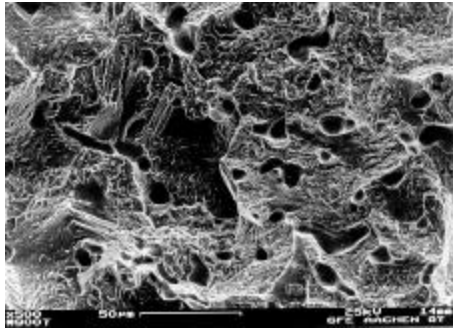
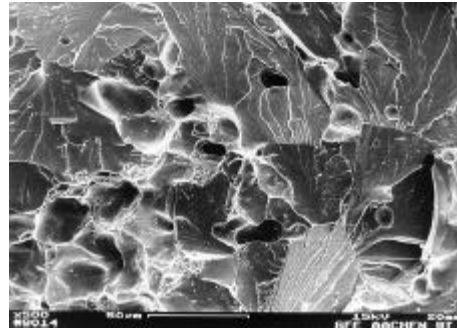
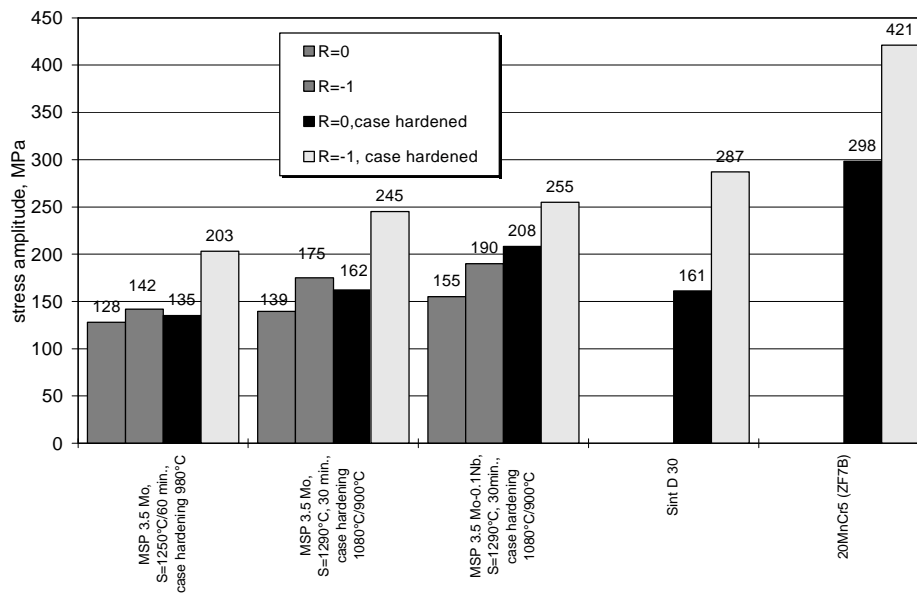


Fig. 12. Reproduction of a fracture in the middle of a case hardened sample (T = RT)



The fatigue strength can be significantly improved both under axial load and under bending stress by changing the microstructure by means of a heat treatment. The surface of the samples is strengthened by case hardening. Besides the hardness profile, there is also a distinctive residual stress profile across the sample cross-section. Normally, residual compressive stresses are present in the case, and residual tensile stresses in the core.

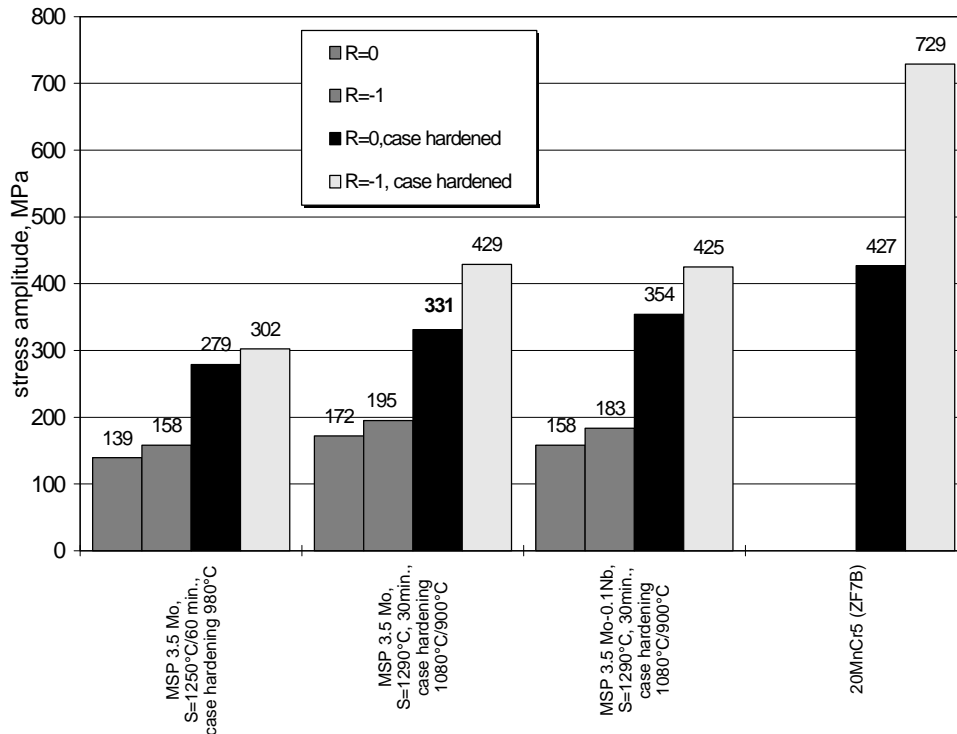
Fig. 13. Fatigue endurance limit ( $P_s=50\%$ ), axial loading



The residual compressive stresses in the case can largely compensate the tensile stresses caused by deflection and axial load. This clearly increases the fatigue endurance limit values. This positive effect particularly manifests itself under bending load, which predominantly acts on the case.

Raising the austenitising temperature from 980°C to 1080°C (to prevent carbide formation at the grain boundaries) improve the fatigue resistance in the case hardened condition, see figure 14. The highest fatigue strengths are reached by the variant MSP 3.5 Mo+0.1Nb. The niobium that is dissolved in sintering forms fine niobium carbides together with the carbon added during austenitising, thus additionally increasing the fatigue strength. In spite of the various possibilities to improve the fatigue strength of sintered steels, they do not match the conventionally produced case hardening steel 20MnCr5 (ZF7B). The latter attains 421 MPa under axial load ( $R = -1$ ) and even 729 MPa under bending stress ( $R = -1$ ). The fatigue strength values of 20MnCr5 are approximately 70% higher in both load cases than those of the optimised variant of the sintered steel MSP 3.5 Mo.

Fig. 14. Fatigue endurance limit ( $P_s=50\%$ ), bending load



## 6. Summary

The sintered steel MSP 3.5 Mo was improved with regard to its strength and toughness properties. By optimising the alloying quantities and the heat treatment, its quasistatic strength characteristics as well as its fatigue strength characteristics could be increased significantly. The sintered steel MSP 3.5Mo is characterised by its very high density of 7.5 g/cm<sup>3</sup> as a result of sintering in the  $\alpha$ -phase as well as by a ductile, ferritic microstructure with low strength characteristics. High elongations after fracture and notch impact energy values can be achieved. It was possible to improve tensile strength and fatigue strength in the as-sintered condition slightly in comparison with the original powder MSP 3.5 Mo by adding the microalloying element niobium. Since this does not restrict the ferritic phase, it ensures high density and thus also high toughness.

By case hardening, the fatigue strength characteristics can be considerably improved, as carbon is introduced into the case, where it creates a martensitic microstructure. In addition, niobium carbides precipitate in the variant MSP 3.5 Mo+0.1Nb as a result of the presence of the alloying element carbon, further increasing the fatigue strength. Special case hardening parameters must be selected for the material MSP 3.5 Mo because of its very high molybdenum content, in order to avoid the formation of special grain boundary carbides of the M<sub>6</sub>C type, because those carbides impair toughness characteristics. The austenitising temperature selected must be above 1050°C to prevent the occurrence of special carbides. This was the purpose of the case hardening treatments.

## References

- [1] Lindner, K.-H.; Link, R.: Neue wasserverdünnte Vergütungsstahlpulver für hochfeste und verschleißfeste Sinterstähle im Automobilbau, Stahl und Eisen 114 (1994) No. 8, p. 123/129
- [2] Lindquist, B.: The influence of pores and microstructure on fatigue of P/M-steels, Modern Developments in Powder Metallurgy (1988), Vol. 1, p. 67/82
- [3] Sonsino, C. M.: Fatigue design for powder metallurgy, Powder Metallurgy (1990), Vol. 33, No. 3, p. 235/245
- [4] Straffelini, G.; Fontanari, V.; Molinari, A.: Influence of microstructure on impact behaviour of sintered ferrous materials, Powder Metallurgy (1995), Vol. 38, No. 1, p. 45/51
- [5] Link, R.: Modern pre-alloyed PM steels and advanced process technology, 1998 PM World Congress, Proceedings Vol. 2, p. 596/606
- [6] Böhm, H.: Einführung in die Metallkunde, Mannheim, 1968, p. 83/92
- [7] Schöler, A.: Development of new P/M materials for highly loaded powder transmission components for the automotive industry, interim report, Institute of Ferrous Metallurgy, RWTH Aachen, not published